Available online at www.sciencedirect.com

ScienceDirect

Procedia Computer Science 60 (2015) 671 – 680

Procedia Computer Science

19th International Conference on Knowledge Based and Intelligent Information and Engineering Systems

Verification of smoke detection in video sequences based on spatio-temporal local binary patterns

Margarita Favorskaya*, Anna Pyataeva, Aleksei Popov

Siberian State Aerospace University, 31 Krasnoyarsky Rabochy av., Krasnoyarsk, 660014 Russian Federation

Abstract

The early smoke detection in outdoor scenes using video sequences is one of the crucial tasks of modern surveillance systems. Real scenes may include objects that are similar to smoke with dynamic behavior due to low resolution cameras, blurring, or weather conditions. Therefore, verification of smoke detection is a necessary stage in such systems. Verification confirms the true smoke regions, when the regions similar to smoke are already detected in a video sequence. The contributions are two-fold. First, many types of Local Binary Patterns (LBPs) in 2D and 3D variants were investigated during experiments according to changing properties of smoke during fire gain. Second, map of brightness differences, edge map, and Laplacian map were studied in Spatio-Temporal LBP (STLBP) specification. The descriptors are based on histograms, and a classification into three classes such as dense smoke, transparent smoke, and non-smoke was implemented using Kullback-Leibler divergence. The recognition results achieved 96–99% and 86–94% of accuracy for dense smoke in dependence of various types of LPBs and shooting artifacts including noise.

Peer-review under responsibility of KES International

Keywords: smoke detection; local binary pattern; dynamic texture; clustering; video sequence; surveillance system

1. Introduction

The reliable smoke detection in large and open spaces is referred to the task of urban safety as well as ecological hazards in order to fire efficient control. In the most cases a smoke is a preliminary feature of fire appearance.

* Corresponding author. Tel.: +7-391-291-9240; fax: +7-391-91-9147.
E-mail address: favorskaya@sibsau.ru

Peer-review under responsibility of KES International
doi:10.1016/j.procs.2015.08.205

Computer vision algorithms are being developed to generate reliable prediction of early smoke detection. Enhancements are being made to distinguish between smoke regions and regions that look like smoke. Usually smoke and fire detection are considered as separate issues because of their different dynamic properties and spatial analysis based on snapshots from video sequence[1,2]. Some researchers investigate a smoke – fire – flame appearance as a unified process in outdoor spaces[3]. However, methods are required that can prevent such dangers with high accuracy and low false alarm rates. The last proposition is important due to great variability of shape, color, transparency, turbulence variance, non-stable motion, boundary roughness, and time-varying flicker effect in the boundaries of smoke as well as artifacts during shooting. There are often introduced through low resolution, blurring, and adverse weather conditions. This makes a smoke detection in video sequences still vulnerable to false alarms. The proposed algorithm of smoke verification based on LBPs after preliminary smoke detection in outdoor scenes provides an accurate clustering of smoke regions and recognition of smoke type. Examples include stationary smoke from factory chimneys and dynamically increasing volume of smoke as a reliable feature of a fire beginning.

A conventional approach to smoke detection is to define global motion and chrominance features in a scene and then find local features such as turbulence, transparency, boundaries changes, among others, in regions similar to smoke. Often motion is estimated using block-matching algorithm or optical flow method. Many algorithms recognize smoke using edge analysis in the spatial domain by applying conventional filters and/or fractal concepts. In the frequency domain they could also apply wavelet-based methods. During burning stages, smoke can be white, light gray, dark gray, and black. The property of transparency also changes in the temporal domain. Some algorithms try to discover differences within the background colors. Our approach is based on edge analysis of background objects. That means if edges in a background become more and more blurred, then it is reasonable to suppose that the analyzed region may be a smoke region.

The remainder of this paper is organized as follows. Section 2 describes a brief survey of smoke detection and smoke clustering methods. A smoke representation as a dynamic texture is discussed in Section 3. The proposed algorithm for verification of smoke detection is presented in Section 4. The experimental results are situated in Section 5. Section 6 includes conclusions.

2. Related work

Many video-based smoke and fire/smoke detection systems are designed for the outdoor space[4,5] and tunnels[6]. They are rarely used for indoor space applications[7]. This is explained by good sensors based on ionization or photometry effects in indoor spaces. However, a possibility to include fire/smoke detection automatically as an additional function in conventional surveillance systems is attractive to manufacturers and customers. In general, video-based smoke detection involves the options mentioned below:

- Extraction of regions similar to smoke based on global motion analysis and chrominance features.
- Local feature extraction (turbulence, transparency, boundaries and color changes) in the spatio-temporal domain.
- Classification by Support Vector Machine (SVM) and Artificial Neural Network (ANN) such as NN with Radial-Basis Function, NN with back propagation, and the Histogram Intersection Kernel (HIK).
- Verification in the spatio-temporal domain is required in order to reduce false alarms in complex scenes with cluttered background and lighting artifacts.

Calderara et al.[8] provided good state-of-the-art smoke detection in large indoor environments such as storehouses and outdoor spaces. Their method is based on wavelet transform energy functions as well as image color properties. For classification, a Bayesian approach was applied with adaptation of a likelihood function to energy ratio and color information. The authors reported that a detection rate of smoke events achieved 100% but the false alarm rate was one event every two weeks during the day and two events every three days during the night surveillance conditions. In work[9], Histograms of Oriented Gradients (HOGs) and Histograms of oriented Optical Flow (HOFs) were constructed in order to build the spatio-temporal descriptor for each “smoke” block from five neighboring frames. Then the SVM classifying was done. These investigations were continued by Ko et al.[10] and Barmpoutis et al.[11]. In order to improve the smoke detection accuracy, Yang and Zheng[12] proposed to use the Adaboost algorithm for smoke detection and classifier based on back propagation in NN. The Adaboost algorithm uses multiple NNs as a set

of strong classifiers. The topology structure of each NN includes 22 input nodes, 22 hidden nodes, and one output node. This approach provided an accuracy rate of 95.66% and false positive rate of 8.62%.

To overcome the problems of arbitrary shapes of smoke, intra-class variations, occlusions and clutter, a double mapping framework was proposed to extract partition based features with the AdaBoost algorithm[13]. The first mapping was based on a feature vector as the concatenating histograms of edge orientation, edge magnitude and the LBP, color intensity, and saturation. As a result, many multi-scale partitions are generated by changing block sizes and partition schemes in order to obtain the shape-invariant features. The second mapping was built using statistical features (mean, variance, skewness, kurtosis, and Hu moments) calculated from block features. Then the AdaBoost algorithm was used to select the discriminative shape-invariant features from a feature pool.

Vidal-Calleja and Agammenoni[14] introduced the unsupervised classifier of unstable smoke patterns, which simultaneously created a codebook and categorized the smoke using a bag-of-words paradigm, based on the Latent Dirichlet Allocation (LDA) model. In experiments, 151 ground truth segmented images with a total number of 97,370 features were prepared. The precision of smoke and non-smoke regions detection using the LDA classification method achieved 67.12% and 95.33%, respectively.

The brief survey demonstrates different approaches. One can see the best results, when smoke is considered as a dynamic texture with the special properties in the spatio-temporal domain.

3. Smoke as a dynamic texture

Smoke and fire can be detected using Dynamic Textures (DTs) even in static scenes under wind rendering in natural environment. In recent years, the study of the DTs attracts attention and interest in order to model and classify such complicated non-rigid gaseous objects. The main difference in DT from static texture connects with dynamic motion behavior, and substance such as smoke possess weakly predicted motion in the temporal domain because of simultaneous influences of many external factors.

The DT recognition methods can be conditionally categorized in the generative, motion field, and discriminative methods. The generative methods simulate the underlying physical dynamic system or phenomenon with visualization of DT sequences. Saisan et al.[15] considered an image sequence with dynamic texture (foliage, water, ocean waves, and smoke) as a realization of a second-order stationary stochastic process under the assumption that the joint statistics between two time instants are shift-invariant. In order to provide a simple statistical description in the space of models, a class of probability densities on the Stiefel manifold was introduced. Three distances were used to estimate the principal angles between specific subspaces, Martin distance, and geodesic distance. Chan and Vasconcelos[16] introduced a term “kernel dynamic texture” as a kernel based on the principal component analysis and studied the DT representation as a non-linear dynamic system. Peteri and Chetverikov[17] show that the normal flow field contains both temporal and structural information about the DTs, and the temporal regularity features (motion patterns) can be used to classify the DTs. The classification without explicit modeling of the underlying dynamic system is in the basis of discriminative methods. Zhao and Pietikainen[18] modeled the DTs by Volume Local Binary Patterns (VLBP) with the co-occurrences on Three Orthogonal Planes (LBP-TOP) in order to make the approach computationally simple and easy to extend. The local texture descriptors based on the VLBP were applied in facial image analysis due to their robustness to challenges such as pose and illumination changes. Ravichandran et al.[19] proposed a collection of Linear Dynamics Systems (LDSs) describing the dynamics of spatio-temporal video patches of the DTs and built the Bag of Systems (BoSs) representation similar to the Bag of Features (BoFs) representation.

The recent works demonstrate some prevalence to the discriminative methods in comparison to other categories for the DT classification. As pointed by Xu et al. in research[20], the main advantage of discriminative methods lies in their robustness to environmental changes and view changes. Xu et al. considered the DT sequences as the sequences, which are generated by some non-linear stochastic dynamic systems with certain inherent multi-scale self-similarities. Four measures were introduced:

- Pixel intensity $\mu_I(p_0, t_0)$ provided by Eq. 1, where $I(p, t)$ is an intensity value of pixel p in time instant t in the sequence $I(\cdot, t)$, $B(p_0, t_0, r_s, r_t)$ is a 3D cube centering at point (p_0, t_0) with spatial radius r_s and temporal radius r_t.

$$\mu_I(p_0,t_0) = \iint_{B(p_0,t_o,r_s,r_t)} I(p,t)\,dp\,dt \tag{1}$$

- Temporal brightness gradient $\mu_B(p_0, t_0)$ as a summation of temporal intensity changes in DT around the point (p_0, t_0) provided by Eq. 2, where $B(p_0, t_0, r_s)$ is a spatial square centering at point (p_0, t_0) with spatial radius r_s.

$$\mu_B(p_0,t_0) = \iint_{B(p_0,t_o,r_s)} \frac{\partial I(p,t)}{\partial t}\,dp \tag{2}$$

- Normal flow $\mu_F(p_0, t_0)$ measures a motion of pixels along the direction perpendicular to the brightness gradient, edge motion as an appropriate measure for chaotic motion of the DTs. This measure can be calculated using Eq. 3.

$$\mu_F(p_0,t_0) = \iint_{B(p_0,t_o,r_s)} \frac{\partial I(p,t)/\partial t}{\|\nabla I(p)\|}\,dp \tag{3}$$

- Laplacian $\mu_L(p_0, t_0)$ means the information of the local co-variance of pixel intensity at point (p_0, t_0) in the spatial-temporal domain (Eq. 4).

$$\mu_L(p_0,t_0) = \iint_{B(p_0,t_o,r_s)} \Delta I(p,t)\,dp \tag{4}$$

Measures represented by Eqs. 1–4 characterize the DT as stochastic dynamic systems with self-similarity in the spatio-temporal domain and can be successful used for smoke verification.

4. Verification of smoke detection

It is reasonable to provide a texture classification by use distributions of simple texture measures like absolute gray level differences, center-symmetric auto-correlation, or the LBPs. Nowadays, the last technique is commonly used. LBP theory is a rapid developed direction, which becomes the overgrown hierarchy of the LBP types for various applications[21]. The basic concepts of the LBPs in 2D and 3D variants are located in Section 4.1. The proposed algorithm is discussed in Section 4.2. A descriptor of smoke regions is represented in Section 4.3 while the classification rule is situated in Section 4.4.

4.1. Basic concepts of local binary patterns

Assume that a texture patch in a gray image $I(x, y)$ is described by the joint distribution T of $(P + 1)$ pixels, where $P > 0$ as it is shown in Eq. 5.

$$T = t(g_c, g_0, g_1, \ldots, g_{P-1}) \tag{5}$$

After subtracting the central pixel value from the neighborhood, one may suppose that the central pixel value is independent on the differences, and Eq. 5 can be factorized in a following manner:

$$T \approx t(g_c)\,t(g_0 - g_c, g_1 - g_c, \ldots, g_{P-1} - g_c). \tag{6}$$

The first factor $t(g_c)$ as an intensity distribution in central pixel contains no useful information while the second factor as the joint distribution differences $t(g_0 - g_c, g_1 - g_c, \ldots, g_{P-1} - g_c)$ can be used to model the local texture.

However, the reliable estimation of such multi-dimensional distribution can be difficult. The solution of this problem based on a vector quantization was proposed by Ojala et al.[22]. The generic LBP operator is derived from this joint distribution.

The LBP was introduced by Ojala et al.[23] as a binary operator robust to lighting variations with low computational cost and ability of simple coding of neighboring pixels around the central pixel as a binary string or decimal value. The operator $LBP(N, R)$ is calculated in a surrounding relative to a central pixel with intensity I_c by Eq. 7, where N is a number of pixels in the neighborhood, R is a radius. If $(I_n - I_c) \geq 0$, then $s(I_n - I_c) = 1$, otherwise $s(I_n - I_c) = 0$.

$$LBP(N,R) = \sum_{n=0}^{N-1} s\left(I_n - I_c\right) \cdot 2^n \tag{7}$$

Pietikäinen et al.[24] categorized the LBPs in texture analysis/classification//recognition/retrieval as mentioned in Table 1 (the main ones).

Table 1. Summary of different LBP types suitable for texture analysis/classification/recognition/retrieval.

Categories	LBP	Short description	Purpose
Preprocessing	Local Edge Patterns (LEP)	Edge detection before LBP computation is used	Retrieval
Thresholding & encoding	Median Binary Patterns (MBP)	The median value within the neighborhood is used for thresholding	Classification
	Soft/Fuzzy LBP	Thresholding is replaced by a fuzzy membership function	Analysis
	Bayesian LBP (BLBP)	Labeling is modeled as a probability and optimization process	Retrieval
Multiscale analysis	Pyramid-based multi-structure LBP	The LBP is applied on different layers of image pyramid	Analysis
	Sparse multi-scale LBP	The discriminative capacity of multi-scale features is exploited	Recognition
Handling rotation	Adaptive LBP (ALBP)	Directional statistical information is incorporated	Classification
	LBP variance (LBPV)	Build rotation variant LBP histogram and apply a global matching	Classification
Handling color	Color vector LBP	Compute the considering pixels as color vectors	Classification
Descriptors	Completed LBP (CLBP)	Use local difference sign-magnitude transform	Classification
Feature selection	Dominant LBP	Make use of the most frequently occurred patterns of LBP	Classification
	Extended LBP	Analyze the structure and probability of non-uniform patterns	Analysis

4.2. The proposed algorithm

Two main versions of 3D LBP, known as the VLBP and the STLBP, exist and are applied in different fields such as background modeling, sign language recognition, and facial expression recognition. The VLBPs sometimes called as Local Binary Patterns from Three Orthogonal Planes (LBP-TOP) analyze information from three orthogonal XY, XT, and YT planes, where T is a time axis[25]. The VLBP is computationally simple and easy to extend. This operator concatenates the LBP co-occurrence statistics in these three directions. However, information in some pixels can repeat and is taken into account twice. The STLBP gathers information from adjacent frames relative the central pixel. For description of the DTs, it is necessary to introduce 3D cuboid of information, thus the application of the STLBP is reasonable. The STLBP becomes voluminous and poorly representative against to generic LBP. However, this is a single way to follow the dynamic properties of the DT in video sequence as it is realized in many methods of motion estimation. The 2D generic and 3D STLBPs in spatial domain and in spatio-temporal domain, respectively, are depicted in Fig. 1 (the green dot means a central pixel).

The main idea is to apply the STLBP technique not only to original image as a set of Intensity Values Map (IVM) but to Temporal brightness Gradient Map (TGM), Normal Flow Map (NFM), and Laplacian Map (LPM), which can be calculated using Eqs. 2–4.

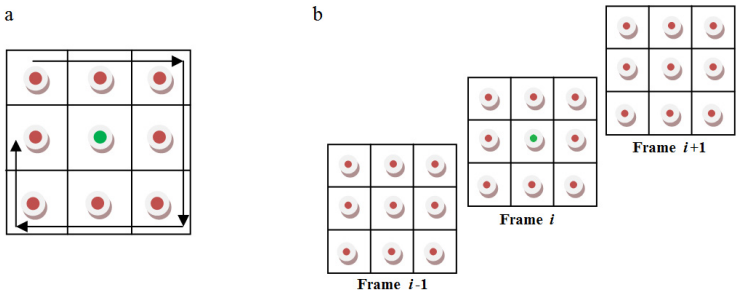

Fig. 1. (a) generic LBP in spatial domain (R = 1); (b) STLBP in spatio-temporal domain (R = 1)

The generalized algorithm is listed using the following steps.

- Step 1. Convert the input image into a grayscale image.
- Step 2. Calculate a current binary map (the IVM, the TGM, the NFM, or the LPM).
- Step 3. Apply the STLBP technique to the current map.
- Step 4. Build a set of local descriptors for the analyzed region.
- Step 5. Apply a histogram approach for classification and store the results.
- Step 6. Repeat Steps 2–5 in a cycle.
- Step 7. Compare the efficiency of the IVM, the TGM, the NFM, or the LPM implementations.
- Step 8. Specify recommendations about the IVM, the TGM, the NFM, or the LPM implementations for analyzed smoke cluster.

This algorithm can use the patterns with pixel sub-sampling and the patterns in every pixel. For patterns with pixel sub-sampling, an image is divided in patches based on a value R, as it is represented in Fig. 2. Each patch is a square with sizes $dim = (2R+1) \times (2R+1)$ pixels, if $R = 1$, then dim = 3 × 3 pixels. If $R = 2$, then dim = 5 × 5 pixels. Thus, the patterns do not intersect. Sometimes, pixels are not enough to fill a patch near image boundaries. Pixels included in a column with width less than $2R$ or a row with a height of less than $2R$ are rejected. The test database involves images with minimum size 300 × 400 pixels and general size 787 × 576 pixels. Thus, the remaining region is no more than 3%, which is not significant for rejection. Another approach is to fill the remaining region with zero values so they will not affect the histogram.

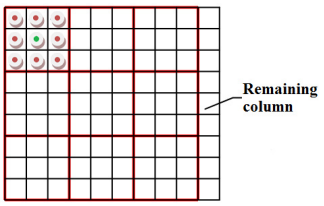

Fig. 2. pattern with pixel sub-sampling (R = 1)

If the patterns in every pixel are built, then the patterns are intersected, and a binary string of the LBP is calculated for each pixel. Both approaches do not influence the calculation of the chosen type of the LBP.

4.3. Descriptor of smoke regions

In this research, a histogram approach was chosen in order to classify the smoke regions because it simplest and fast. For some types of the LBP, a preliminary processing for histogram building is required. Classic LBPs do not

need pre-processing. The uniform LBPs, which include not more than three transitions from 0 to 1 and vise versa[21], are invariant for rotation and determine spots, the ends of lines, angles, and planes. The uniform LBP can be represented as a list of cycle shifts. A number is assigned to each cycle shift, and this number is considered as an invariant to rotation. Then a binary list is transformed to decimal list. Finally, a result histogram is built classically. The ternary LBPs require the high LBP, where negative values are changed by 1, and the low LBP, where negative values are replaced by 0. Then two histograms are built based on high and low LBPs.

Two ways are known for histogram building using a set of n-bits binary codes:

- Classical approach, when each binary line is transformed in decimal number and then amount of equal numbers is calculated defining a position and a height of histogram columns.
- Alternative approach, when a sum of 1 is calculated for each bit of LBP and then a height of histogram columns is determined.

4.4. Classification of smoke regions

Chi-square distance, histogram intersection distance, Kullback-Leibler (KL) divergence, and G-statistic are often used during classification. In this research, the KL divergence was chosen for histogram comparison as it is recommended frequently in literature.

The Kullback-Leibler (KL) divergence as a generalization of Shannon's entropy is a relative entropy measure, not a true metric. It can be adapted for measuring distances between histograms in order to analyze the probability of occurrence of code numbers for compared textures[26]. First, the probability of occurrence of the code numbers is accumulated into one histogram per image. Each bin in a histogram represents a code number. Second, the constructed histograms of test images are normalized. Third, the KL divergence is computed by Eq. 8, where $h \in 1, 2$ is a number of compared histograms $H(\cdot)$ and K is the total number of coded numbers.

$$D_{KL} = \sum_{h=1}^{2}\sum_{j=1}^{K} H(h,j)\log H(h,j) - \sum_{j=1}^{K} H_p(j)\log H_p(j) \qquad H_p(j) = \sum_{h=1}^{2} H(h,j) \tag{8}$$

The results of these calculations are discussed in Section 5.

5. Experimental results

For experimental researches, the database of dynamic textures Dyntex was used†. Three video sequences with dense smoke and one video sequence with transparent smoke from this database were applied with manual extraction of following fragments:

- 660 fragments of dense smoke with sizes 70 × 70 pixels.
- 83 fragments of transparence smoke with sizes 55 × 65 pixels.
- 991 fragments without smoke with sizes 70 × 70 pixels.
- 336 fragments without smoke with sizes 55 × 65 pixels.

The patterns calculated in each pixel are preferable with higher True Recognition (TR) values and low estimates of False Rejection Rate (FRR) and False Acceptance Rate (FAR). The comparative evaluations for dense smoke/non-smoke fragments and transparent smoke/non-smoke fragments for various types of the LBPs (the best results) are situated in Tables 2 and 3, respectively. During experiments the classical approach of building histograms was applied because it provides better results than the alternative methods used.

---

† http://projects.cwi.nl/dyntex/

Table 2. Recognition results of dense smoke fragments (TR, FRR, and FAR, %).

Video fragments	TR	FRR	FAR	TR	FRR	FAR	TR	FRR	FAR
	2D LBP			2D Ternary LBP			2D Uniform LBP		
	$R = 1$								
Dense smoke fragments	99.7	0.58	0.30	99.8	1.91	0.27	99.8	0.46	0.21
Non-smoke fragments	99.5	0.34	0.62	98.1	0.23	1.70	99.2	0.32	0.48
	2D extended LBP								
	$R = 1$			$R = 2$					
	8 neighbouring points			8 neighbouring points			12 neighbouring points		
Dense smoke fragments	99.8	0.25	0.13	99.8	2.50	0.24	99.4	1.98	0.20
Non-smoke fragments	99.8	0.18	0.22	97.4	0.16	2.12	97.9	0.21	1.43
	3D extended LBP (STLBP)								
	$R = 1$			$R = 2$					
	8 neighbouring points			8 neighbouring points			12 neighbouring points		
Dense smoke fragments	99.0	0.70	1.04	98.5	0.64	1.50	98.5	0.30	1.50
Non-smoke fragments	99.4	0.02	0.60	92.6	0.52	0.18	99.9	0.21	0.16

For dense smoke (Table 2), the true recognition has high value for all types of the LBPs reaching 100% in the case of the STLBP. 2D extended LBP, $R = 1$ demonstrates better results in FRR and FAR estimates than 2D LBP, 2D ternary LBP, and 2D uniform LBP, $R = 1$. 2D extended LBP, $R = 2$ provides the similar TR values, however, FRR and FAR estimates are worse. During all experiments, the STLBP application ensured the best estimates.

Table 3. Recognition results of transparent smoke fragments (TR, FRR, and FAR, %).

Video fragments	TR	FRR	FAR	TR	FRR	FAR	TR	FRR	FAR
	2D LBP			2D Ternary LBP			3D Ternary LBP		
	$R = 1$								
Transparent smoke fragments	75.9	30.1	24.1	77.1	25.8	22.9	74.4	46.0	25.6
Non-smoke fragments	68.5	29.9	31.5	73.5	22.1	26.5	49.0	38.5	51.0
	2D extended LBP								
	$R = 1$			$R = 2$					
	8 neighbouring points			8 neighbouring points			12 neighbouring points		
Transparent smoke fragments	95.2	3.60	4.80	74.7	31.7	25.3	69.9	36.3	30.1
Non-smoke fragments	96.7	2.60	3.30	66.7	36.1	33.3	62.2	28.7	37.8
	3D extended LBP (STLBP)								
	$R = 1$			$R = 2$					
	8 neighbouring points			8 neighbouring points			12 neighbouring points		
Transparent smoke fragments	67.1	66.2	32.9	56.1	59.7	43.9	59.8	57.1	40.2
Non-smoke fragments	25.7	23.1	74.3	36.4	52.1	63.6	38.8	41.6	61.2

2D LBPs, 2D/3D ternary LBPs, and 3D extended LBPs do not provide the appropriate results in the case of transparent smoke (Table 3). Maximum value of true recognition achieves 95.2% with FRR = 3.6% and FAR = 4.8% in 2D case. Thus, a single method for recognition of transparent smoke can be recommended: 2D extended LBPs, $R = 1$. This is explained by a background blurring in scene with a transparent smoke. This experiment shows that when R value increases, the accuracy decreases.

The results from both Tables 2–3 were obtained for the original images without being transformed into gradient maps. According to the proposed numerical methodology, some results were obtained for images, which were previously processed by gradient maps (Eqs. 1–4). As an example, Table 4 includes the best results for Laplacian map. In the most case of LBPs for dense smoke, Laplacian filter provides non-significant improvement up 1–2% better. 3D extended LBPs, $R = 1$ and 8 neighbouring points and $R = 2$ and 12 neighbouring points, increase the accuracy decreasing FRR and FAR estimates. In the case of transparent smoke, the accuracy was decreased to 78%.

Table 4. Recognition results of dense and transparent smoke fragments processed by Laplacian (TR, FRR, and FAR, %).

Video fragments	TR	FRR	FAR	TR	FRR	FAR	TR	FRR	FAR
	3D extended LBP (STLBP)								
	$R = 1$			$R = 2$					
	8 neighbouring points			8 neighbouring points			12 neighbouring points		
Dense smoke fragments	98.5	0.30	1.50	98.5	0.30	1.50	98.5	0.50	1.50
Non-smoke fragments	100	0.10	0.00	100	0.20	0.00	99.7	0.40	0.30
Transparent smoke fragments	62.2	42.9	37.8	64.6	33.8	35.4	48.8	60.4	51.2
Non-smoke fragments	55.8	35.2	44.2	66.6	34.1	33.4	37.3	59.8	62.7

Also some artifacts were tested. The images were blurred by Gaussian filter. The recognition results are worse on 1–2% and 5–10% for dense and transparent smoke, respectively, for 3D extended LBPs. This means that the additional deblurring methods are required before recognition stage. Experiments with white Gaussian noise demonstrated that ternary and extended LPBs are robust to such distortions. As an example, Table 5 shows results for dense smoke recognition in the case of 3D extended LBPs with 0.3, 0.5, and 0.8 dB, respectively.

Table 5. Recognition results of dense smoke fragments with noise (TR, FRR, and FAR, %).

Video fragments	TR	FRR	FAR	TR	FRR	FAR	TR	FRR	FAR
	3D extended LBP (STLBP)								
	$R = 1$			$R = 2$					
	8 neighbouring points			8 neighbouring points			12 neighbouring points		
Dense smoke fragments (0.3 dB)	99.5	2.40	0.50	99.0	2.00	1.00	99.0	1.30	1.00
Non-smoke fragments (0.3 dB)	97.2	2.10	2.80	97.8	1.20	2.20	98.6	1.20	1.40
Dense smoke fragments (0.5 dB)	98.5	3.10	1.50	99.0	0.70	1.00	99.5	5.90	0.50
Non-smoke fragments (0.5 dB)	96.6	2.10	3.40	99.4	0.60	0.60	92.9	0.40	7.10
Dense smoke fragments (0.8 dB)	87.7	20.6	12.3	97.1	3.80	2.90	95.1	10.0	4.90
Non-smoke fragments (0.8 dB)	77.7	14.5	22.3	96.1	4.00	3.90	89.0	5.00	11.0

2D extended LBPs do not suitable for transparent smoke. 3D extended LBPs are acceptable especially with $R = 1$. Value $R = 2$ provides sparse calculation with worse evaluations. The shooting artifacts under noise decrease the accuracy of dense and transparent smoke to 86–94%.

6. Conclusion

In this research, a verification of dense smoke, transparent smoke, and non-smoke regions is solved using various types of the LBPs. The idea of STLBP building based on map of brightness differences, edge map, and Laplacian map was investigated, and the promising results was received. The pattern in every pixel provides accurate results than the pattern with pixel sub-sampling. Experiments show that ternary LBPs are robust to noise, and 3D extended LBPs are the best for texture analysis of smoke providing 100% of accuracy for dense smoke and 96% of accuracy

for transparent smoke, when a pattern radius is equal 1. These results verify that both 2D and 3D extended LBPs detect lines, angles, and planes, even in blurred images.

References

1. Feiniu Y. A fast accumulative motion orientation model based on integral image for video smoke detection, *Pattern Recognition Letters* 2008;**29(7)**:925-932.
2. Vipin V. Image Processing Based Forest Fire Detection, *Int J of Emerging Technology and Advanced Engineering* 2012;**2(2)**:87-95.
3. Celik, T., Ozkaramanly, H., Demirel, H. "Fire and Smoke Detection Without Sensors: Image Processing Based Approach," 15th European Signal Processing Conference. Poznan, Poland, 2007, 1794-1798.
4. Favorskaya M, Levtin K. Early Smoke Detection in Outdoor Space by Spatio-Temporal Clustering Using a Single Video Camera. In: Tweedale JW, Jain LC, editors. *Recent Advances in Knowledge-based Paradigms and Applications*, Advances in Intelligent Systems and Computing, vol. 234, Switzerland: Springer International Publishing; 2014, p. 43-56.
5. Lee CY, Lin CT, Hong CT, Su MT. Smoke Detection Using Spatial and Temporal Analyses. *Int J of Innovative Computing, Information and Control* 2012;**8(6)**:1-11.
6. Han D, Lee B. Flame and Smoke Detection Method for Early Real-Time Detection of a Tunnel Fire. *Fire Safety Journal* 2009;**44(7)**:951-961.
7. Dukuzumuremyi JP, Zou B, Hanyurwimfura D. A Novel Algorithm for Fire/Smoke Detection based on Computer Vision. *Int J of Hybrid Information Technology* 2014;**7(3)**:143-154.
8. Calderara S, Piccinini P, Cucchiara R. Vision based smoke detection system using image energy and color information. *Machine Vision and Applications* 2011;**22(4)**:705-719.
9. Avgerinakis, K., Briassouli, A., Kompatsiaris, I. "Smoke Detection Using Temporal HOGHOF Descriptors and Energy Colour Statistics from Video," International Workshop on Multi-Sensor Systems and Networks for Fire Detection and Management Firesense Workshop, Antalya, Turkey, 2012, p. 3-8.
10. Ko BC, Park JO, Nam JY. Spatiotemporal bag-of-features for early wildfire smoke detection. *Image and Vision Computing* 2013;**31(10)**:786-795.
11. Barmpoutis, P., Dimitropoulos, K., Grammalidis, N. "Smoke Detection Using Spatio-Temporal Analysis, Motion Modeling and Dynamic Texture Recognition," 22nd European Signal Processing Conference, Lisbon, Portugal, 2014, p. 1078-1082.
12. Yang S, Zheng X. A Video Smoke Detection Method Based on Various Features Integration and Adaboost. *J of Computational Information Systems* 2014;**10(24)**:10463-10471.
13. Yuan F. A double mapping framework for extraction of shape-invariant features based on multi-scale partitions with AdaBoost for video smoke detection. *Pattern Recognition* 2012;**45(12)**:4326-4336.
14. Vidal-Calleja, T.A., Agammenoni, G. "Integrated Probabilistic Generative Model for Detecting Smoke on Visual Images," IEEE International Conference on Robotics and Automation River Centre, Saint Paul, Minnesota, USA, 2012, p. 2183-2188.
15. Saisan, P., Doretto, G., Wu, Y., Soatto, S. "Dynamic texture recognition," IEEE Computer Society Conference on Computer Vision and Pattern Recognition, Kauai, HI, USA, 2001, p. 58-63.
16. Chan, A., Vasconcelos, N. "Classifying Video with Kernel Dynamic Textures," IEEE Conference on Computer Vision and Pattern Recognition, Minneapolis, MN, USA, 2007, p. 1-6.
17. Peteri R, Chetverikov D. Dynamic Texture Recognition Using Normal Flow and Texture Regularity. In: Marques JS, de la Blanca NP, Pina P, editors. *Pattern Recognition and Image Analysis*. LNCS vol. 3523, Berlin, Heidelberg: Springer-Verlag; 2005, p. 223-230.
18. Zhao G, Pietikainen M. Dynamic texture recognition using local binary patterns with an application to facial expression. *IEEE Trans PAMI* 2007;**29(6)**:915-928.
19. Ravichandran, A., Chaudhry, R., Vidal, R. "View-invariant dynamic texture recognition using a bag of dynamical systems," IEEE Conference on Computer Vision and Pattern Recognition, Miami, FL, USA, 2009, p. 1651-1657.
20. Xu, Y., Quan, Y., Ling, H., Ji, H. "Dynamic Texture Classification Using Dynamic Fractal Analysis," IEEE International Conference on Computer Vision, Barcelona, Spain, 2011, p. 1219-1226.
21. Brahnam S, Jain LC, Nanni L, Lumini A. Local Binary Patterns: New Variants and Applications. *Studies in Computational Intelligence*, vol. 506. Berlin Heidelberg: Springer-Verlag; 2014.
22. Ojala T, Valkealahti K, Oja E, Pietikäinen M. Texture discrimination with multidimensional distributions of signed gray-level differences. *Pattern Recognition* 2001;**34(3)**:727-739.
23. Ojala T, Pietikäinen M, Harwood D. A comparative study of texture measures with classification based on feature distributions. *Pattern Recognition* 1996;**29**:51–59.
24. Pietikäinen M., Hadid, A., Zhao, G., Ahonen, T. Computer Vision Using Local Binary Patterns. *Computational Imaging and Vision*, vol. 40, Springer-Verlag London Limited; 2011.
25. Zhao G, Pietikäinen M. Dynamic Texture Recognition Using Volume Local Binary Patterns. In: Vidal R, Heyden A, Ma Y (eds) *Dynamical Vision*. LNCS vol. 4358, 2007, 165–177.
26. Ojala, T., Pietikainen, M., Harwood, D. "Performance Evaluation of Texture Measures with Classification Based on Kullback Discrimination of Distributions," 12th IAPR International Conference on Pattern Recognition, vol. 1 - Conference A: Computer Vision & Image Processing, Jerusalem, Israel, 1994, p. 582–585.